Path-integral Monte Carlo simulations without the sign problem: Multilevel blocking approach for effective actions

R. Egger,[1] L. Mühlbacher,[1,2] and C. H. Mak[2]

[1]*Fakultät für Physik, Albert-Ludwigs-Universität, D-79104 Freiburg, Germany*
[2]*Department of Chemistry, University of Southern California, Los Angeles, California 90089-0482*

The multilevel blocking algorithm recently proposed as a possible solution to the sign problem in path-integral Monte Carlo simulations has been extended to systems with long-ranged interactions along the Trotter direction. As an application, results for the real-time quantum dynamics of the spin-boson model are presented.

PACS number(s): 02.70.Lq, 05.30.−d, 05.40.−a

I. INTRODUCTION

Path-integral Monte Carlo (PIMC) simulations are useful for extracting exact results on many-body quantum systems [1]. In principle, PIMC methods can be used to study both equilibrium and dynamical problems. But in the cases of fermions and real-time dynamics, the PIMC method suffers from the notorious ''sign problem'' which renders such simulations unstable. This sign problem manifests itself as an exponential decay of the signal-to-noise ratio for large systems or long real times [2–4]. Its origin is at the heart of quantum mechanics itself, namely, the interference of different quantum paths contributing to the path integral might be destructive due to exchange effects or due to the oscillatory nature of the real-time evolution operator. Expect for approximate treatments [2], the sign problem has remained unsolved.

Very recently, a new strategy was proposed as a possible approach to a complete solution of the sign problem. This so-called multilevel blocking (MLB) algorithm [5,6] is a systematic implementation of the simple blocking idea—by sampling ''blocks'' instead of single paths, one can *always* reduce the sign problem [7]. Defining a suitable hierarchy of blocks by grouping them into different ''levels,'' crucial information about the phase cancellations among different quantum paths can then be recursively transferred from the bottom level to the top level. Given sufficient computer memory, such an approach was shown to be able to eliminate the sign problem in a stable and exact manner [5]. But to date, the MLB algorithm has only been formulated to solve the sign problem in PIMC simulations with nearest-neighbor interactions along the Trotter direction. This situation is encountered under a direct Trotter-Suzuki breakup of the short-time propagator.

In this paper, we report an extension of the MLB approach to the case of effective actions that may include arbitrarily long-ranged interactions. Such effective actions, that are nonlocal in Trotter time, may arise from degrees of freedoms having been traced out, e.g., a harmonic heat bath [8], or through a Hubbard-Stratonovich transformation, e.g., in auxiliary-field MC simulations of lattice fermions [3]. Remarkably, because such effective actions capture much of the physics, e.g., symmetries or the dissipative influence of the

traced-out degrees of freedom, the corresponding path integral very often exhibits a significantly reduced ''intrinsic'' sign problem compared to the original (time-local) formulation. The present generalization of the MLB algorithm was developed to take advantage of this fact. We note that in a PIMC simulation with only nearest-neighbor interactions along the Trotter direction, the original MLB approach [5] is more efficient than the method described below, which therefore should be used only for time-non-local actions.

To be specific, we focus on the dynamical sign problem arising in real-time PIMC computations here. The modifications required to implement the method for fermion simulations are then straightforward. The structure of this paper is as follows. In Sec. II the general strategy to deal with long-ranged interactions in a MLB scheme is outlined. A detailed exposition of the computational method can be found in Sec. III. We have studied the real-time dynamics of the celebrated spin-boson system [8] using this approach. Details about this application, performance issues related to the sign problem, and numerical results are presented in Sec. IV. Finally, Sec. V offers some conclusions.

II. GENERAL CONSIDERATIONS

We consider a discretized path integral along a certain contour in the complex-time plane. In a typical real-time calculation, there is a forward branch from $t=0$ to $t=t^*$, where t^* is the maximum time studied in the simulation, followed by a branch going back to the origin, and then by an imaginary-time branch from $t=0$ to $t=-i\hbar\beta$. We focus on a ''factorized'' initial preparation where the relevant degrees of freedom, denoted by $r(t)$, are held fixed for $t<0$ [8,9]. That implies that the imaginary-time dynamics must be frozen at the corresponding value, and we only need to sample on the two real-time branches. Note that such a nonequilibrium calculation cannot proceed in a standard way by first doing an imaginary-time quantum Monte Carlo simulation followed by an analytic continuation of the numerical data [1]. The quantum numbers $r(t)$ at a given time may be discrete or continuous variables.

Using time slices of length t^*/P, we combine forward $[r(t_m)]$ and backward $[r'(t_m)]$ path configurations at time

$t_m = mt^*/P$ into the configuration s_m, where $m = 1, \ldots, P$. The configuration at $t = 0$ is held fixed, and for $t = t^*$ we must be in a diagonal state, $r(t^*) = r'(t^*)$. For an efficient application of the current method, it is essential to combine several neighboring slices m into new ''blocks.'' For instance, think of $m = 1, \ldots, 5$ as a new ''slice'' $l = 1$, $m = 6, \ldots, 10$ as another slice $l = 2$, and so on. Combining q elementary slices into a block s_l, instead of the original P slices we have $L = P/q$ blocks, where L is the number of MLB ''levels.'' In actual applications, there is considerable freedom in how these blocks are defined, e.g., if there is hardly any intrinsic sign problem, or if there are only few variables in r, one may choose larger values of q. Additional flexibility can be gained by choosing different q for different blocks.

Say we are interested in sampling the configurations s_L on the top level $l = L$ according to the appropriate matrix elements of the (reduced) density matrix,

$$\rho(s_L) = Z^{-1} \sum_{s_1, \ldots, s_{L-1}} \exp\{-S[s_1, \ldots, s_L]\}, \quad (2.1)$$

where S is the effective action under study and Z is a normalization constant so that

$$\sum_{s_L} \rho(s_L) = 1. \quad (2.2)$$

Due to the time-non-locality of this action, there will be interactions among all blocks s_l. The sum in Eq. (2.1) denotes either an integration over continuous degrees of freedom or a discrete sum. In the case of interest here, the effective action is complex valued, and $e^{-S}/|e^{-S}|$ represents an oscillatory phase factor (± 1 for the fermion sign problem). The ''naive approach'' to the sign problem is to sample configurations using the positive definite weight function

$$\mathcal{P} \sim |\exp\{-S\}|, \quad (2.3)$$

and to include the oscillatory phase in the accumulation procedure. This leads precisely to the exponentially fast decay of the signal-to-noise ratio with t^*.

The proposed MLB simulation scheme starts by sampling $l = 1$ on the finest level, so only variables in the first block corresponding to $m = 1, \ldots, q$ are updated. During this procedure, interference among different paths will take place. Since only relatively few degrees of freedom are sampled, however, the resulting interference information can be quantified in a controlled way by employing so-called ''level-l bonds'' (here $l = 1$). As long as q is chosen sufficiently small, the interference cannot lead to numerical instabilities, and the sign cancellations occurring while sampling on level $l = 1$ can thus be synthesized and transferred to the level $l = 2$, where the sampling is carried out next. Here the procedure is repeated, and, by proceeding recursively up to the top level $l = L$, this strategy can eliminate the sign problem. The main bottleneck of the method comes from the immense memory requirements, since one needs to store and update the level-l bonds on all levels during the Monte Carlo sampling (see below for details). To summarize, the main idea of our approach is to subdivide the allowed interferences among the quantum paths into small subunits (blocks) such that no sign problem occurs when (stochastically) summing over the paths within each subunit. The basic observation underlying our method is therefore almost trivial: The sign problem does not occur in a sufficiently small system. The nontrivial computational task then consists of bringing together the interference signals from different blocks, which is done by recursively forming blocks on subsequent higher levels.

Instead of the ''circular'' structure of the time contour inherent in the trace operation, it is actually more helpful to view the problem as a linear chain, where the proposed MLB scheme proceeds from left to right. In the case of local actions with only nearest-neighbor interactions along Trotter time, a different recursion scheme was implemented in Refs. [5,6] which is close in spirit to the usual block-spin transformations used in renormalization group treatments of spin chains. For both MLB implementations, however, the underlying blocking idea is identical, and the nonlocality of the effective action studied here only requires one to abandon block-spin-like transformations in favor of the ''moving-along-the-chain'' picture.

Below we assume that one can decompose the effective action according to

$$S[s_1, \ldots, s_L] = \sum_{l=1}^{L} W_l[s_l, \ldots, s_L]. \quad (2.4)$$

All dependence on a configuration s_l is then contained in the ''partial actions'' W_λ with $\lambda \leq l$. One could, of course, put all $W_{l>1} = 0$, but the approach becomes more powerful if a nontrivial decomposition is possible.

III. MULTILEVEL BLOCKING APPROACH

In the following, we describe in detail how the MLB algorithm for effective actions is implemented in practice. The MC sampling starts on the finest level $l = 1$, where only the configuration $s_{l=1}$ containing the elementary slices $m = 1, \ldots, q$ will be updated with all $s_{l>1}$ remaining fixed at their initial values s_l^0. Using the weight function

$$\mathcal{P}_0[s_1] = |\exp\{-W_1[s_1, s_2^0, \ldots, s_L^0]\}|,$$

we generate K samples $s_1^{(i)}$, where $i = 1, \ldots, K$, and store them for later use. To effectively solve the sign problem and to avoid a bias in the algorithm, the sample number K should be chosen large enough; see below and in Ref. [5]. For $K = 1$, the algorithm simply reproduces the naive approach.

The stored samples are now employed to generate information about the sign cancellations. All knowledge about the interference that occured at this level is encapsulated in the quantity

$$B_1 = \left\langle \frac{\exp\{-W_1[s_1, \ldots, s_L]\}}{|\exp\{-W_1[s_1, s_2^0, \ldots, s_L^0]\}|} \right\rangle_{\mathcal{P}_0[s_1]}$$

$$= C_0^{-1} \sum_{s_1} \exp\{-W_1[s_1, \ldots, s_L]\}$$

$$= K^{-1} \sum_{i=1}^{K} \frac{\exp\{-W_1[s_1^{(i)}, s_2, \ldots, s_L]\}}{|\exp\{-W_1[s_1^{(i)}, s_2^0, \ldots, s_L^0]\}|} = B_1[s_2, \ldots, s_L],$$

$$(3.1)$$

which we call ''level-1 bond'' in analogy to Ref. [5], with the normalization constant $C_0 = \Sigma_{s_1} P_0[s_1]$. The third line follows by noting that the $s_1^{(i)}$ were generated according to the weight P_0. This equality requires that K is sufficiently large and that q is sufficiently small in order to provide a good statistical estimate of the level-1 bond.

Combining the second expression in Eq. (3.1) with Eq. (2.1), we rewrite the density matrix in the following way:

$$\rho(s_L) = Z^{-1} \sum_{s_2, \ldots, s_{L-1}} \exp\left\{-\sum_{l>1} W_l\right\} C_0 B_1$$

$$= Z^{-1} \sum_{s_1, \ldots, s_{L-1}} P_0 B_1 \prod_{l>1} e^{-W_l}. \quad (3.2)$$

When comparing Eq. (3.2) with Eq. (2.1), we see that the entire sign problem has now formally been transferred to levels $l>1$, since oscillatory phase factors only arise when sampling on these higher levels. Note that $B_1 = B_1[s_2, \ldots, s_L]$ introduces couplings among *all* levels $l > 1$, in addition to the ones already contained in the effective action S.

We now proceed to the next level $l=2$ and, according to Eq. (3.2), update configurations for $m = q+1, \ldots, 2q$ using the weight

$$P_1[s_2] = |B_1[s_2, s_3^0, \ldots, s_L^0] \exp\{-W_2[s_2, s_3^0, \ldots, s_L^0]\}|. \quad (3.3)$$

Under the move $s_2 \rightarrow s_2'$, we should then resample and update the level-1 bonds, $B_1 \rightarrow B_1'$. Exploiting the fact that the stored K samples $s_1^{(i)}$ are correctly distributed for the original configuration s_2^0, the updated bond can be computed according to

$$B_1' = K^{-1} \sum_{i=1}^{K} \frac{\exp\{-W_1[s_1^{(i)}, s_2', \ldots, s_L]\}}{|\exp\{-W_1[s_1^{(i)}, s_2^0, \ldots, s_L^0]\}|}. \quad (3.4)$$

Again, to obtain an accurate estimate for B_1', the number K should be sufficiently large. In the end, sampling under the weight P_1 implies that the probability for accepting the move $s_2 \rightarrow s_2'$ under the Metropolis algorithm is

$$p = \left| \frac{\sum_i \dfrac{\exp\{-W_1[s_1^{(i)}, s_2', s_3^0, \ldots]\}}{|\exp\{-W_1[s_1^{(i)}, s_2^0, \ldots]\}|}}{\sum_i \dfrac{\exp\{-W_1[s_1^{(i)}, s_2, s_3^0, \ldots]\}}{|\exp\{-W_1[s_1^{(i)}, s_2^0, \ldots]\}|}} \right|$$
$$\times \left| \frac{\exp\{-W_2[s_2', s_3^0, \ldots]\}}{\exp\{-W_2[s_2, s_3^0, \ldots]\}} \right|. \quad (3.5)$$

Using this method, we generate K samples $s_2^{(i)}$, store them, and compute the level-2 bonds,

$$B_2 = \left\langle \frac{B_1[s_2, s_3, \ldots] \exp\{-W_2[s_2, s_3, \ldots]\}}{|B_1[s_2, s_3^0, \ldots] \exp\{-W_2[s_2, s_3^0, \ldots]\}|} \right\rangle_{P_1[s_2]}$$

$$= C_1^{-1} \sum_{s_2} B_1[s_2, \ldots] \exp\{-W_2[s_2, \ldots]\}$$

$$= K^{-1} \sum_{i=1}^{K} \frac{B_1[s_2^{(i)}, s_3, \ldots] \exp\{-W_2[s_2^{(i)}, s_3, \ldots]\}}{|B_1[s_2^{(i)}, s_3^0, \ldots] \exp\{-W_2[s_2^{(i)}, s_3^0, \ldots]\}|}$$

$$= B_2[s_3, \ldots, s_L], \quad (3.6)$$

with $C_1 = \Sigma_{s_2} P_1[s_2]$. Following our above strategy, we then rewrite the reduced density matrix by combining Eq. (3.2) and the second line of Eq. (3.6). This yields

$$\rho(s_L) = Z^{-1} \sum_{s_3, \ldots, s_{L-1}} \exp\left\{-\sum_{l>2} W_l\right\} C_0 C_1 B_2$$

$$= Z^{-1} \sum_{s_1, \ldots, s_{L-1}} P_0 P_1 B_2 \prod_{l>2} e^{-W_l}. \quad (37)$$

Clearly, the sign problem has been transferred one block further to the right along the chain. Note that the normalization constants $C_0, C_1, \ldots$ depend only on the initial configuration s_l^0 so that their precise values need not be known.

This procedure is now iterated in a recursive manner. Sampling on level l using the weight function

$$P_{l-1}[s_l] = |B_{l-1}[s_l, s_{l+1}^0, \ldots] \exp\{-W_l[s_l, s_{l+1}^0, \ldots]\}| \quad (3.8)$$

requires the recursive update of all bonds B_λ with $\lambda < l$. Starting with $B_1 \rightarrow B_1'$ and putting $B_0 = 1$, this recursive update is done according to

$$B_\lambda' = K^{-1} \sum_{i=1}^{K}$$

$$\times \frac{B_{\lambda-1}'[s_\lambda^{(i)}, s_{\lambda+1}, \ldots] \exp\{-W_\lambda'[s_\lambda^{(i)}, s_{\lambda+1}, \ldots]\}}{|B_{\lambda-1}[s_\lambda^{(i)}, s_{\lambda+1}^0, \ldots] \exp\{-W_\lambda[s_\lambda^{(i)}, s_{\lambda+1}^0, \ldots]\}|}, \quad (3.9)$$

where the primed bonds or partial actions depend on s_l' and the unprimed ones on s_l^0. Iterating this to get the updated bonds B_{l-2} for all $s_{l-1}^{(i)}$, the test move $s_l \rightarrow s_l'$ is then accepted or rejected according to the probability

$$p = \left| \frac{B_{l-1}[s_l', s_{l+1}^0, \ldots] \exp\{-W_l[s_l', s_{l+1}^0, \ldots]\}}{B_{l-1}[s_l, s_{l+1}^0, \ldots] \exp\{-W_l[s_l, s_{l+1}^0, \ldots]\}} \right|. \quad (3.10)$$

On this level, we again generate K samples $s_l^{(i)}$, store them, and compute the level-l bonds according to

$$B_l[s_{l+1}, \dots] = K^{-1} \sum_{i=1}^{K} \frac{B_{l-1}[s_l^{(i)}, s_{l+1}, \dots] \exp\{-W_l[s_l^{(i)}, s_{l+1}, \dots]\}}{|B_{l-1}[s_l^{(i)}, s_{l+1}^0, \dots] \exp\{-W_l[s_l^{(i)}, s_{l+1}^0, \dots]\}|}. \tag{3.11}$$

This process is iterated up to the top level, where the observables of interest may be computed.

Since the sampling of B_l requires the resampling of all lower-level bonds, the memory and CPU requirements of the algorithm laid out here are quite large. For $\lambda < l-1$, one needs to update $B_\lambda \rightarrow B_\lambda'$ for all $s_{l'}^{(i)}$, with $\lambda < l' < l$, which implies a tremendous amount of computer memory and CPU time, scaling approximately $\sim K^L$ at the top level. Fortunately, an enormous simplification can often be achieved by exploiting the fact that the interactions among distant slices are usually weaker than between nearby slices. For instance, when updating level $l=3$, the correlations with the configurations $s_1^{(i)}$ may be very weak, and instead of summing over all K samples $s_1^{(i)}$ in the update of the bonds $B_{\lambda < l}$, we may select only a small subset. When invoking this argument, one should be careful to also check that the additional interactions coming from the level-λ bonds with $\lambda < l$ are sufficiently short ranged. From the definition of these bonds, this is to be expected though.

Remarkably, this algorithm can significantly relieve the severity of the sign problem. Let us first give a simple qualitative argument supporting this statement for the original MLB method of Ref. [5], where $P=2^L$, with L denoting the number of levels. If one needs K samples for each slice on a given level in order to have satisfactory statistics despite the sign problem, the total number of paths needed in the naive approach depends exponentially on P, namely, $\sim K^P$. This is precisely the well-known exponential severity of the sign problem under the naive approach. However, with the MLB method the work on the last level [which is the only one affected by a sign problem provided K was chosen sufficiently large] is only $\sim K^L$. So in the MLB method, the work needed to sample the K^P paths with satisfactory statistical accuracy grows $\sim K^{\ln_2 P} = P^{\ln_2 K}$, i.e., only algebraically with P. Provided the interactions along the Trotter time decay sufficiently fast, a similar qualitative argument can be given for the generalized MLB algorithm proposed here. For the application described below, we have indeed found only algebraic dependences of the required CPU times and memory resources with the maximum real time t^*, instead of exponential ones as encountered in the naive approach. Further details of the simulation procedure are provided in Sec. IV

IV. APPLICATION: SPIN-BOSON DYNAMICS

To demonstrate this MLB algorithm for path-integral simulations with long-range interactions in the Trotter direction, we study the real-time dynamics of the spin-boson model;

$$H = -(\hbar\Delta/2)\sigma_x + (\hbar\epsilon/2)\sigma_z$$
$$+ \sum_\alpha \left[\frac{p_\alpha^2}{2m_\alpha} + \tfrac{1}{2} m_\alpha \omega_\alpha^2 \left(x_\alpha - \frac{c_\alpha}{m_\alpha \omega_\alpha^2} \sigma_z \right)^2 \right]. \tag{4.1}$$

This archetypal model has a number of important applications, e.g., the Kondo problem, interstitial tunneling in solids [8], quantum computing [10], and electron transfer reactions [11], to mention only a few. The bare two-level system (TLS) has a tunneling matrix element Δ and an asymmetry (bias) ϵ between the two localized energy levels (σ_x and σ_z are Pauli matrices). Dissipation is introduced via a linear heat bath, i.e., an arbitrary collection of harmonic oscillators $\{x_\alpha\}$ bilinearly coupled to σ_z. Concerning the TLS dynamics, all information about the coupling to the bath is contained in the spectral density $J(\omega) = (\pi/2) \Sigma_\alpha (c_\alpha^2/m_\alpha \omega_\alpha) \delta(\omega - \omega_\alpha)$, which has a quasicontinuous form in typical condensed-phase applications. $J(\omega)$ dictates the form of the (twice-integrated) bath correlation function ($\beta = 1/k_B T$):

$$Q(t) = \int_0^\infty \frac{d\omega}{\pi\hbar} \frac{J(\omega)}{\omega^2} \frac{\cosh[\omega\hbar\beta/2] - \cosh[\omega(\hbar\beta/2 - it)]}{\sinh[\omega\hbar\beta/2]}. \tag{4.2}$$

For the calculations here, we assume an ohmic spectral density of the form $J(\omega) = 2\pi\hbar\alpha\omega\exp(-\omega/\omega_c)$, for which $Q(t)$ can be found in closed form [7]. Here ω_c is a cutoff frequency, and the damping strength is measured by the dimensionless Kondo parameter α. In the scaling limit $\Delta \ll \omega_c$, and assuming $\alpha < 1$, all dependence on ω_c enters via a renormalized tunnel splitting [8]

$$\Delta_{\text{eff}} = [\cos(\pi\alpha)\Gamma(1-2\alpha)]^{1/2(1-\alpha)} (\Delta/\omega_c)^{\alpha/(1-\alpha)} \Delta, \tag{4.3}$$

and powerful analytical [8,12] and alternative numerical methods [13,14] are available for computing the nonequilibrium dynamics.

At this point some remarks are in order. Basically all other published numerical methods except the real-time PIMC method can deal only with equilibrium quantities; see, e.g., Refs. [15,16], or explicitly introduce approximations [13,14,17,18]. Regarding the latter class, mostly Markovian-type approximations concerning the time range of the interactions introduced by the influence functional have been implemented. Our approach is computationally more expensive than other methods [13–18], but at the same time it is unique in yielding numerically exact results for the nonequilibrium spin-boson dynamics for arbitrary bath spectral densities. It is particularly valuable away from the scaling regime where important applications, e.g., coherent (nonequilibrium) electron transfer reactions in the adiabatic regime, are found but basically all other methods fail to yield exact results. Finally we briefly compare the present approach to our previously published PIMC method [7]. For not exceedingly small α, it turns out that the latter method is just equivalent to the $K=1$ limit of the present method. From Table I and the discussion below, it is thus apparent that the

TABLE I. MLB performance for $\alpha = 1/2$, $\omega_c/\Delta = 6$, $\Delta t^* = 10$, $P = 40$, and several L. q_l denotes the number of slices for $l = 1, \ldots, L$.

K	L	q_l	$\langle \text{sgn} \rangle$
1	1	40	0.03
200	2	30–10	0.14
800	2	30–10	0.20
200	3	22–12–6	0.39
600	3	22–12–6	0.45

MLB method is significantly more powerful in allowing for a study of much longer real times than previously.

We study the quantity $P(t) = \langle \sigma_z(t) \rangle$ under the nonequilibrium initial preparation $\sigma_z(t < 0) = +1$. $P(t)$ gives the time-dependent difference of the quantum-mechanical occupation probabilities of the left and right states, with the particle initially confined to the left state. To obtain $P(t)$ numerically, we take the discretized path-integral representation of Ref. [7], and trace out the bath to obtain a long-ranged effective action; the ''influence functional.'' In discretized form the TLS path is represented by spins $\sigma_i, \sigma_i' = \pm 1$ on the forward and backward paths, respectively. The total action S consists of three terms. First, there is the ''free'' action S_0 determined by the bare TLS propagator U_0:

$$\exp(-S_0) = \prod_{i=0}^{P-1} U_0(\sigma_{i+1}, \sigma_i; t^*/P) U_0(\sigma_{i+1}', \sigma_i'; -t^*/P).$$

(4.4)

The second is the influence functional $S_I = S_I^{(1)} + S_I^{(2)}$, which contains the long-ranged interaction among the spins,

$$S_I^{(1)} = \sum_{j \geq m} (\sigma_j - \sigma_j')\{L_{j-m}'(\sigma_m - \sigma_m') + i L_{j-m}''(\sigma_m + \sigma_m')\},$$

(4.5)

where $L_j = L_j' + i L_j''$ is given by [7]

$$L_j = [Q((j+1)t^*/P) + Q((j-1)t^*/P) - 2Q(jt^*/P)]/4$$

(4.6)

for $j > 0$, and $L_0 = Q(t^*/P)/4$. In the scaling regime at $T = 0$, this effective action has interactions $\sim \alpha/t^2$ between the spins (''inverse-square Ising model''). The contribution

$$S_I^{(2)} = i(t^*/P) \sum_m \gamma(mt^*/P)(\sigma_m - \sigma_m')$$

(4.7)

gives the interaction with the imaginary-time branch [where $\sigma_z = +1$], where the damping kernel

$$\gamma(t) = \frac{2}{\pi \hbar} \int_0^\infty d\omega \frac{J(\omega)}{\omega} \cos(\omega t).$$

(4.8)

For clarity, we focus on the most difficult case of an unbiased two-state system at zero temperature, $\epsilon = T = 0$. To ensure that the Trotter error is negligibly small, we have systematically increased P for fixed t^* until convergence was
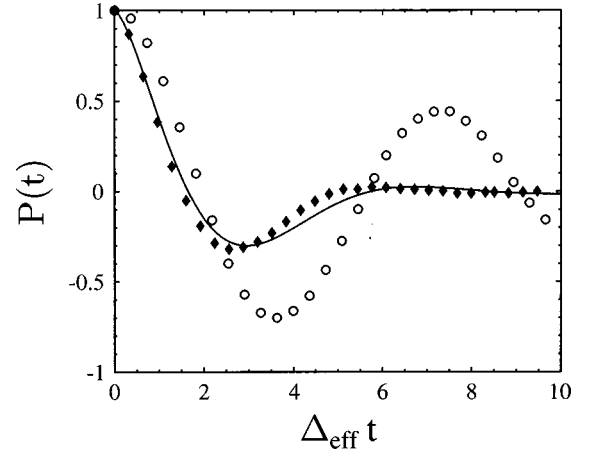

FIG. 1. Scaling curves for $P(t)$ for $\alpha = 1/4$ with $\omega_c/\Delta = 6$ (closed diamonds) and $\omega_c/\Delta = 1$ (open circles). The solid curve is the NIBA prediction. The approach of Ref. [7] becomes unstable for $\Delta_{\text{eff}} t > 4$ in both cases. Statistical errors are of the order of the symbol sizes.

reached. Typical CPU time requirements per 10^4 MC samples are 4 h for $P = 26$, $L = 2$, and $K = 1000$, or 6 h for $P = 40$, $L = 3$, and $K = 600$, where the simulations were carried out on SGI Octane workstations. The memory requirements for these two cases are 60 and 160 Mbyte, respectively. Data were collected from several 10^5 samples.

For $\alpha = 0$, the bare TLS dynamics $P(t) = \cos(\Delta t)$ is accurately reproduced. As mentioned above, the performance is slightly inferior to the original MLB approach [6], which is now applicable due to the absence of the influence functional and the associated long-ranged interactions. Turning to the situation where a bath is present, we first study the cases $\alpha = 1/2$ and $\omega_c/\Delta = 6$. The exact $\alpha = 1/2$ result [8], $P(t) = \exp(-\Delta_{\text{eff}} t)$, valid in the scaling regime $\omega_c/\Delta \gg 1$, was accurately reproduced, indicating that the scaling regime is reached already for moderately large ω_c/Δ. Typical parameters used in the MLB simulations and the respective average sign are listed in Table I. The first line in Table I corresponds to the naive approach. For $\alpha = 1/2$, it turns out that our previous PIMC scheme [7] yields a comparable performance to the $K = 1$ version of this MLB method. It is then clear from Table I that the average sign and hence the signal-to-noise ratio can be dramatically improved thus allowing for a study of significantly longer time scales t^* than before. For a fixed number of levels L, the average sign grows by increasing the parameter K. Alternatively, for fixed K, the average sign increases with L. Evidently, the latter procedure is more efficient in curing the sign problem, but at the same time computationally more expensive. In practice, it is then necessary to find a suitable compromise.

Figure 1 shows scaling curves for $P(t)$ at $\alpha = 1/4$ for $\omega_c/\Delta = 6$ and $\omega_c/\Delta = 1$. According to the $\alpha = 1/2$ results, $\omega_c/\Delta = 6$ is expected to be within the scaling regime. This is confirmed by a comparison to the noninteracting blip approximation (NIBA) [8]. The minor deviations of the NIBA curve from the exact result are in accordance with Refs. [7,12] for $\alpha \leq 1/2$. However, for $\omega_c/\Delta = 1$, scaling concepts (and also the NIBA) are expected to fail even qualitatively. Clearly, the MLB results show that away from the scaling region, quantum coherence is able to persist for much longer,

and both frequency and decay rate of the oscillations differ significantly from the predictions of the NIBA. In electron transfer reactions in the adiabatic-to-nonadiabatic crossover regime, such coherence effects can then strongly influence the low-temperature dynamics. One obvious and important consequence of these coherence effects is the breakdown of a rate description, implying that theories based on an imaginary-time formalism might not be appropriate in this regime. A detailed analysis of this crossover regime using the MLB method is currently in progress.

V. CONCLUSIONS

In this paper, we have extended the multilevel blocking (MLB) approach of Refs. [5,6] to path-integral Monte Carlo simulations with long-ranged effective actions along the Trotter direction. For clarity, we have focused on real-time simulations here, but believe that a similar approach can also be helpful in many-fermion computations, e.g., in auxiliary-field fermion simulations of lattice fermions. The practical usefulness of the approach was demonstrated by computing the nonequilibrium real-time dynamics of the dissipative two-state system. Here the effective action (influence func-tional) arises by integrating out the linear heat bath. For a heat bath of the ohmic type, at $T=0$ the corresponding interactions among different time slices decay only with a slow inverse-square power law.

In the present implementation of the MLB method, the basic blocking idea operates on multiple time scales by carrying out a subsequent sampling at longer and longer times. During this procedure, the interference information collected at shorter times is taken fully into account without invoking any approximation. Under such an approach, at the expense of large memory requirements, the severity of the sign problem can be significantly relieved. The proposed approach allows one to study time scales not accessible to previous real-time path-integral simulations for the spin-boson system.

---

[1] See, e.g., *Quantum Monte Carlo Methods in Condensed Matter Physics,* edited by M. Suzuki (World Scientific, Singapore, 1993), and references therein.

[2] D.M. Ceperley and B.J. Alder, Science **231**, 555 (1986).

[3] E.Y. Loh, Jr., J. Gubernatis, R.T. Scalettar, S.R. White, D.J. Scalapino, and R.L. Sugar, Phys. Rev. B **41**, 9301 (1990).

[4] D. Thirumalai and B.J. Berne, Annu. Rev. Phys. Chem. **37**, 401 (1986).

[5] C.H. Mak, R. Egger, and H. Weber-Gottschick, Phys. Rev. Lett. **81**, 4533 (1998).

[6] C.H. Mak and R. Egger, J. Chem. Phys. **110**, 12 (1999).

[7] R. Egger and C.H. Mak, Phys. Rev. B **50**, 15 210 (1994); for a review, see C.H. Mak and R. Egger, Adv. Chem. Phys. **93**, 39 (1996).

[8] A.J. Leggett, S. Chakravarty, A.T. Dorsey, M.P.A. Fisher, A. Garg, and W. Zwerger, Rev. Mod. Phys. **57**, 1 (1987); U. Weiss, *Quantum Dissipative Systems* (World Scientific, Singapore, 1993), and references therein.

[9] The calculation of thermal correlation functions is possible after minor modifications.

[10] A. Garg, Phys. Rev. Lett. **77**, 964 (1996).

[11] D. Chandler, in *Liquids, Freezing, and the Glass Transition*, Les Houches Lectures, edited by D. Levesque, J.P. Hansen, and J. Zinn-Justin (Elsevier Science, North-Holland, 1991).

[12] F. Lesage and H. Saleur, Phys. Rev. Lett. **80**, 4370 (1998).

[13] J. Stockburger and C.H. Mak, Phys. Rev. Lett. **80**, 2657 (1998).

[14] D. Makarov and N. Makri, Chem. Phys. Lett. **221**, 482 (1994).

[15] T.A. Costi and C. Kieffer, Phys. Rev. Lett. **76**, 1683 (1996); T.A. Costi, *ibid.* **80**, 1038 (1998).

[16] K. Völker, Phys. Rev. B **58**, 1862 (1998).

[17] M. Winterstetter and W. Domcke, Chem. Phys. Lett. **236**, 445 (1995).

[18] H. Wang, X. Song, D. Chandler, and W.H. Miller, J. Chem. Phys. **110**, 4828 (1999).